

Electron density in the sodium vanadium oxide bronze β - $\text{Na}_x\text{V}_2\text{O}_5$ at 9 K

Ruslan P. Ozerov,^{a*} Victor A. Streltsov,^b Alexander N. Sobolev,^c Brian N. Figgis^c and Victor L. Volkov^d

^aMendeleev University of Chemical Technology of Russia, 125047 Moscow, Russia,

^bCrystallography Centre, The University of Western Australia, Nedlands 6907, Australia,

^cDepartment of Chemistry, The University of Western Australia, Nedlands 6907, Australia,

and ^dInstitute of Solid State Chemistry, 620219 Ekaterinburg, Russia

Correspondence e-mail: ozerov@muctr.edu.ru

Received 18 September 2000

Accepted 30 January 2001

The crystal structure and electron density in sodium vanadium oxide bronze, β - $\text{Na}_x\text{V}_2\text{O}_5$ [$x = 0.282(3)$], have been studied by accurate Mo $K\alpha$ X-ray diffraction measurements at 9.6(3) K. No noticeable difference in the crystal structures at room temperature and 9.6 K has been observed. No superstructure reflections, previously found by Kanai, Kagoshima & Nagasawa [(1982), *J. Phys. Soc. Jpn.*, **51**, 697–698], have been detected at low temperature. Analysis of the deformation electron density has revealed the presence of the quasi-two-dimensional sheets of the $-\text{V}-\text{O}-\text{V}-\text{O}-$ bonds in the structure. The electron density in the different chemical bonds within each of the three crystallographically independent VO_6 polyhedra noticeably varies, although there is no clear evidence that the three crystallographically independent V atoms have different valence states.

1. Introduction

The triple metal oxides $nM_2O \cdot mV_2O_4 \cdot pV_2O_5$ with $M = \text{Li}, \text{Na}, \text{K}, \text{Ag}$ and Cu used to be known as the vanadico vanadates (Cannari & de Pava, 1936). It was later found that the Na and K isomorphous compounds crystallize in the oxide-type monoclinic phase (Wadsley, 1955; Ozerov *et al.*, 1957) named later as a β -phase. The V atoms form deformed VO_6 octahedra with common edges and corners. They form a rigid cage with tunnels spread along the unique b axis. The M atoms are disposed in the tunnels of that cage. Owing to the observed high anisotropy of the electric conductivity of the β -phase single crystal in the monoclinic y -axis direction, found by Ozerov (1957) and further confirmed by Wallis *et al.* (1977), these crystals are now considered to be quasi-one-dimensional conductors. Since these compounds exhibit other quite unique physical (electrical, optical, mechanical *etc.*) and chemical (high resistance to acids) properties, the heading 'bronzes' has been suggested for such compounds (Ozerov, 1954) due to their similarity to tungsten bronzes (Ozerov, 1955).

The sodium isomorph is the most studied β -phase. There are six $\text{Na}_{0.33}\text{V}_2\text{O}_5$ 'molecules' in the unit cell. Three different types of V atoms, the Na atom and seven different O atoms occupy the $4i$ (m) crystallographic positions in the unit cell (space group No. 12, $C2/m$). The Na-atom positions are approximately half occupied. The eighth O atom is in the $2a$ ($2/m$) position with fixed parameters. The perspective view of the crystal structure is depicted in Fig. 1. Highly distorted VO_6 polyhedra form a rigid framework with Na atoms located inside the continuous tunnels along the monoclinic y axis. Fig. 2

presents the V_3O_{14} (a) and Na_2O_{10} (b) fragments of the structure, the sequence of the VO_6 polyhedra of different types is given in Fig. 2(c). The polyhedra around V3 atoms are deformed more than others and are often considered as a quadratic pyramid, as presented in Fig. 2(c). The M crystallographic sites are paired at a distance of ~ 2.0 Å on the $0y0$ plane (Fig. 2b), whereas the distance between two Na atoms along the y axis is 3.6 Å. Considering the metal and ionic radii of the Na atom of 1.89 and 0.98 Å, respectively, the pairing of the Na atoms in the $0y0$ plane in the β -phase is highly unlikely because the distance between them is too short, resulting in strong cation–cation repulsion. In order to avoid very short contacts, three models of the M -atom distribution among four crystallographic sites were proposed (Ozerov, 1957). One of the models suggests the ordered altering of the occupation of the Na sites along the monoclinic axis. This requires the doubling of the b unit-cell parameter. The second model suggests the random altering of the Na sites occupation and no changes of the unit-cell parameters are required. The last model places the Na atoms one under another along the y axis. In all cases, accordingly, the total chemical content of the crystal unit cell is $M_2V_{12}O_{30}$ ($M_{0.33}V_2O_5 \times 6$) rather than $M_4V_{12}O_{30}$, as can be expected from the $C2/m$ space group crystallographic sites.

It is generally believed that the unusual calorimetric, electrical, chemical and magnetic properties originate from the special electronic states of the M and V atoms, and interatomic interactions in the highly distorted coordination polyhedra. In particular, in order to explain the electron conduction anisotropy, the early model suggested delocalization of the valence electrons of the alkali atoms and the formation of a quasi-one-dimensional electron band (Ozerov, 1957, 1959a,b). According to this assumption the alkali metal atoms should have the metallic M^0 valence state.

Later on, another model for the anisotropy was proposed. It was based on the absence of the Knight shift observed in the NMR signals for ^{23}Na (Maruyama & Nagasawa, 1980) and 7Li (Gendell *et al.*, 1962) nuclei, which indicated the absence of free electrons in the crystals. This suggests that alkali atoms should be completely ionized in the host structure, whereas

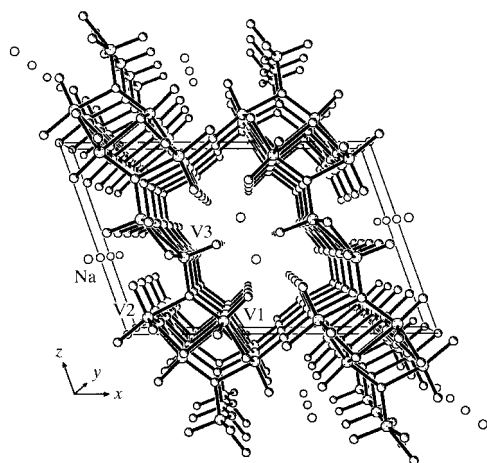


Figure 1
Perspective view of the β -phase crystal structure.

electrons transfer from an alkali atom to the vanadium d -shell creates the V^{4+} ion. The existence of the $V^{4+}-V^{4+}$ spin-singlet pairs (bipolarons) formed by strong electron–phonon coupling was suggested by Chakraverty *et al.* (1978) in order to explain the high quasi-one-dimensional electrical conductivity. The existence of bipolarons was also supported by the anomalous temperature dependence of the ^{51}V Knight shift in the NMR spectra (Onoda *et al.*, 1982), as well as by accurate EPR measurements of the g -shift and signal line-width angular dependence (Takahashi & Nagasawa, 1981). Thus, the anisotropy of the electrical conductivity can be explained by bipolarons travelling along the y axis while the conductivity in the other two perpendicular directions is due to a diffusive electron hopping motion (Onoda & Nagasawa, 1983). In further studies the polaron condensation and the bipolaron ordering phenomena were supposed to be observed by NMR and X-ray diffuse scattering (Nagasawa *et al.*, 1987). The phase transitions detected in the Na-, Cu- and Ag-bronzes were related to bipolaron crystallization (Onoda & Nagasawa, 1987).

It should also be mentioned that certain types of satellite reflections were observed in several alkali bronze β -phases at low temperatures (Kanai *et al.*, 1982), possibly originating from the bipolaron ordering.

The aim of this work is to re-examine the crystal structure and to study the electron density in β - $Na_xV_2O_5$ at low temperature in an attempt to improve our understanding of the chemical bonding in this compound. X-ray diffraction measurements were conducted at room temperature and 9.6 K. The wide temperature range was allowed to check the possible phase transition in this crystal.

2. Experimental

Single crystals were grown from stoichiometric mixtures of V_2O_5 and sodium bicarbonate Na_2CO_3 by the Bridgman method (Volkov, 1987). No special attempts to control the sodium content at the stage of the crystal grown were undertaken. A single crystal sample of rectangular shape bounded by (010), ($\bar{1}01$) and (201) faces with the dimensions $0.210 \times 0.142 \times 0.051$ mm³ was chosen for the X-ray diffraction experiments. All data collection details are presented in Table 1. Crystal faces were measured and indexed using both SEM and optical microscopy. Unit-cell parameters were determined using 12 reflections in the θ range 37.75 – 39.1° . Reflection intensities were measured systematically using $\omega/2\theta$ continuous time scans for a full sphere up to $(\sin \theta/\lambda)_{\max} = 1.0798$ Å⁻¹.

The integrated intensities were recovered from raw scans using the profile-fitting program *PROFIT* (Streltsov & Zavodnik, 1989). Before cooling the sample, a preliminary data measurement for a full sphere up to $\theta = 40^\circ$ was conducted at room temperature.

Integrated intensities were modified and structure-factor variances from counting statistics were adjusted for experimental instability, as indicated by the standards. Lorentz and polarization corrections were applied. Absorption correction

Table 1

Experimental details.

Crystal data	
Chemical formula	Na _{0.282} V ₂ O ₅
Chemical formula weight	188.36
Cell setting, space group	Monoclinic, <i>C2/m</i>
<i>a</i> , <i>b</i> , <i>c</i> (Å)	15.3500 (1), 3.6115 (4), 10.058 (1)
β (°)	109.560 (7)
<i>V</i> (Å ³)	525.40 (9)
<i>Z</i>	6
<i>D_x</i> (Mg m ⁻³)	3.594
Radiation type	Mo <i>K</i> α
No. of reflections for cell parameters	12
θ range (°)	37.75–39.1
μ (mm ⁻¹)	5.254
Temperature (K)	9.6 (3)
Crystal form, colour	Rectangular, black
Crystal size (mm)	0.21 × 0.142 × 0.051
Data collection	
Diffractometer	Huber 512
Data collection method	ω -2 θ scans
Absorption correction	Analytical
<i>T_{min}</i>	0.4731
<i>T_{max}</i>	0.7757
No. of measured, independent and observed parameters	10 461, 2938, 2897
Criterion for observed reflections	$I > 2\sigma(I)$
<i>R_{int}</i>	0.0275
θ_{max} (°)	50
Range of <i>h</i> , <i>k</i> , <i>l</i>	-32 → <i>h</i> → 32 -7 → <i>k</i> → 7 -21 → <i>l</i> → 21
No. and frequency of standard reflections	3 every 100 reflections
Intensity decay (%)	2
Refinement	
Refinement on	<i>F</i>
<i>R</i> , <i>wR</i> , <i>S</i>	0.0156, 0.0111, 1.979
No. of reflections and parameters used in refinement	2897, 253
Weighting scheme	$w = 1/\sigma^2(F)$
Extinction method	Becker & Coppens (1974)

Computer programs used: *XD* (Koritsanzsky *et al.* (1998)).

factors (Alcock, 1974) were evaluated analytically. Symmetrically equivalent reflections were averaged and all of the resulting 2897 unique reflections were used for structural refinements. Variances consistent with measurement statistics were retained and those for the remaining reflections were increased according to the scatter of equivalents following the Fisher test.

Attempts were made to find superstructure reflections at low temperature arising from the *b*-axis doubling reported by Kanai *et al.* (1982). Fig. 3 presents a scan along the 0*y*0 direction measured with high accuracy. Only principal reflections are seen in the scan. Therefore, no *b*-axis doubling was found at the experimental temperature (9.6 K).

3. Least-squares refinements

3.1. Conventional refinement

Independent structural parameters, including the scale factor, fractional coordinates and anisotropic atomic displace-

ment parameters were refined by conventional full-matrix least-squares, including all observed structure factors. The reference state for all structure-factor calculations was the independent atom model (IAM) calculated using spherical atomic scattering factors with dispersion corrections $\Delta f'$, $\Delta f''$ from *International Tables for X-ray Crystallography* (1974, Vol. IV).

The secondary extinction parameter was also estimated as part of the least-squares optimization of the structural model. Zachariasen's (1967) formula was included in the refinement according to Larson (1970). The minimum extinction correction (y_{min}) was 0.84 for the (020) reflection ($F_{obs} = yF_{kin}$, where F_{kin} is the value of the kinematic structure factor). This

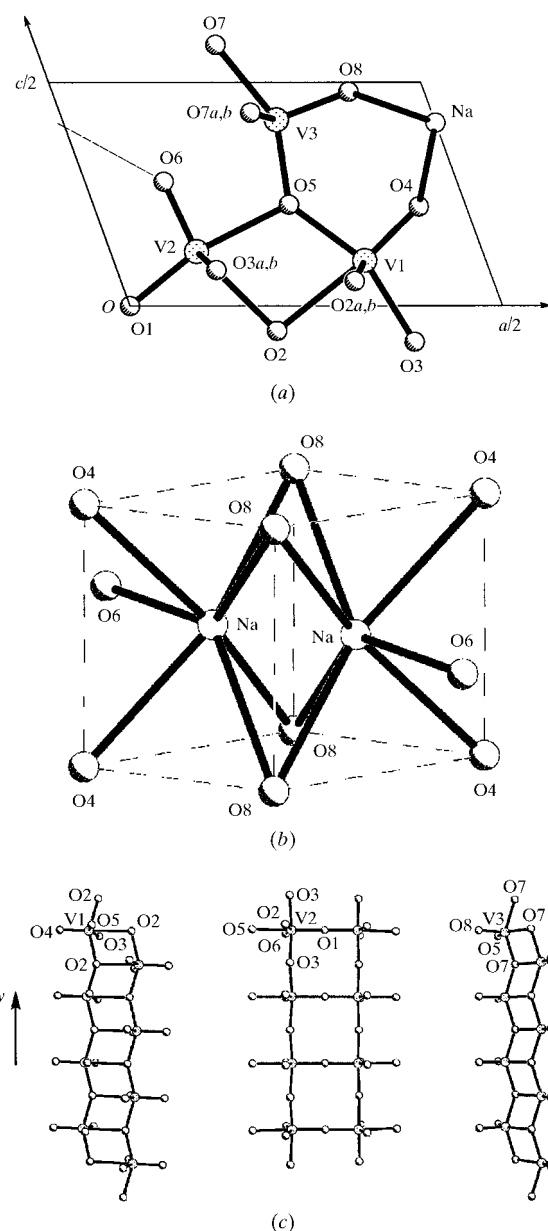


Figure 2
Structural fragments: (a) V₃O₁₄, (b) Na₂O₁₀ and (c) V polyhedral sequence.

refinement converged to $R(F) = 0.0225$, $wR(F) = 0.0241$ and $S = 0.0432$ with sodium content $x = 0.282$ (3).

Further experimental details of the data refinements are given in Table 1. Calculations were based on the *Xtal3.6* system of crystallographic programs (Hall *et al.*, 1999).

3.2. Multipole refinement

Refinement of the multipole model was also attempted. In addition to the scale factor and conventional structural parameters (positional and harmonic anisotropic atomic displacements), pseudo-atomic multipole population parameters up to hexadecapoles ($l = 4$, total 253 parameters) were refined using the *XD* program (Koritzansky *et al.*, 1988). The Becker & Coppens (1974) isotropic secondary extinction (Type 1) parameter using a Gaussian distribution of the mosaic spread was also refined. The minimum extinction correction (y_{\min}) was 0.80 for the (020) reflection. Since all atoms are in special (m) symmetry positions, the crystallographic symmetry

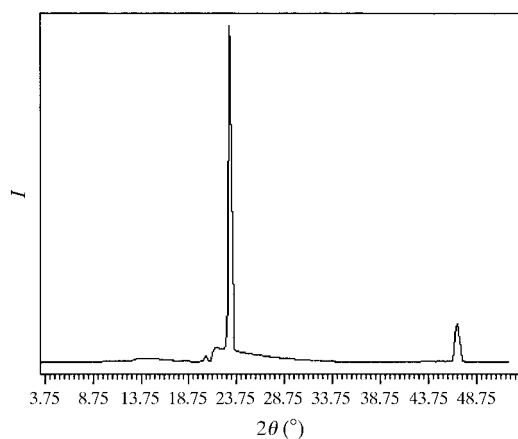


Figure 3
The (0k0) scan.

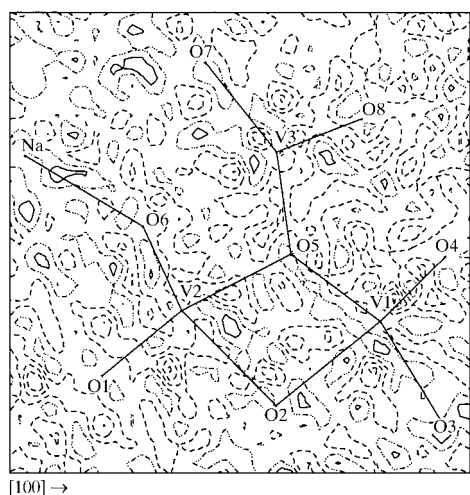


Figure 4
Residual ($F_{\text{obs}} - F_{\text{model}}$) deformation electron density map in the (010) plane. Contour intervals are $0.2 \text{ e } \text{Å}^{-3}$; positive contours are solid and negative contours are shown as short dashed lines. Map borders are $9.5 \times 7 \text{ Å}$.

Table 2

Selected atomic distances (Å).

V1—O2 ⁱ	1.86746 (13)	V3—O5	1.7871 (5)
V1—O2	2.3345 (5)	V3—O6	2.6634 (6)
V1—O3	1.9856 (5)	V3—O7 ⁱⁱ	1.88845 (14)
V1—O4	1.5942 (5)	V3—O7	1.9952 (5)
V1—O5	1.9467 (5)	V3—O8	1.5982 (5)
V2—O1	1.79176 (13)	Na—Na ⁱⁱⁱ	1.9591 (14)
V2—O2	2.3369 (5)	Na—O4 ^{iv}	2.5381 (6)
V2—O3 ⁱ	1.89178 (14)	Na—O6	2.3919 (9)
V2—O5	2.1427 (5)	Na—O8 ⁱⁱⁱ	2.4350 (6)
V2—O6	1.6066 (5)	Na—O8 ^{iv}	2.6319 (6)

Symmetry codes: (i) $\frac{1}{2} - x, \frac{1}{2} + y, -z$; (ii) $\frac{1}{2} - x, \frac{1}{2} + y, 1 - z$; (iii) $-x, y, 1 - z$; (iv) $x - \frac{1}{2}, \frac{1}{2} + y, z$.

constraints were applied to reduce the amount of refined multipole parameters. The expansion–contraction parameters of the pseudo-atomic electron density were also included. Initially, the Na atom was considered neutral. Refinement of this model was unstable, showing higher correlation between parameters. Na atoms were then assumed to be the Na^{1+} ions with the 3s valence orbital population fixed to zero. The residual electrons were distributed over the O atoms to satisfy unit-cell electroneutrality. Refinement of this model was stable and converged to the lowest least-squares indexes: $R(F) = 0.0156$, $wR(F) = 0.0110$ and $S = 0.0198$. The optimization of the Na ion-valence population at the final stage of the multipole refinement resulted in insignificant adjustments of the population parameters and the least-squares indexes. Fig. 4 presents the final residual map. The absence of significant positive and negative peaks indicates that the multipole model refinement was satisfactory.

4. Results and discussion

4.1. *b*-axis doubling

The absence of the superstructure reflections is illustrated in Fig. 3, which is in contradiction to the results of Kanai *et al.* (1982). The disagreement can be attributed to the fact that only two measurements (273 and 9 K) were performed, whereas the doubling could exist in the intermediate temperature range. Moreover, it is also possible that the doubling depends on the sodium content and sample preparation procedure, as recently shown by Yamada & Ueda (1999).

4.2. Atomic coordinates, interatomic distances and electron density

The fractional coordinates and thermal atomic displacement parameters have been deposited,¹ and selected interatomic distances are given in Table 2. Structural parameters do not differ noticeably from those previously reported for the series of isomorphous compounds. There is a large variation in the V—O distances of the VO polyhedra ranging from 1.6 up

¹Supplementary data for this paper are available from the IUCr electronic archives (Reference: AV0034). Services for accessing these data are described at the back of the journal.

Table 3
Charges from the multipole population refinement (in electrons).

V1	+2.03	O3	-0.99
V2	+2.33	O4	-0.85
V3	+1.83	O5	-1.32
Na	+1.00	O6	-0.68
O1	-0.44	O7	-1.08
O2	-0.69	O8	-0.78

to 2.66 Å (Table 3). The shortest vectors are all directed towards the nearest Na atoms at the same (V2—O6··Na) or at the adjacent $b/2$ level (V1—O4··Na and V3—O8··Na). The atomic displacement parameters are rather small, except the U^{22} parameters for the O4 and O8 atoms. All the O atoms mentioned above belong to the nearest neighborhood of the Na atoms (Fig. 2*b*).

The multipole model deformation electron density ($\Delta\rho$) maps are depicted in Figs. 5 and 6. In Fig. 5 the $\Delta\rho$ map in the (010) plane, through all three independent polyhedra along the mirror plane (see Fig. 2*a*), reflects the significant differences in the V—O distances and, consequently, in $\Delta\rho$ topography. There are pronounced electron accumulations, usually attributed to covalent bonding, in the short V2—O6 (1.60 Å) and long V2—O2 (2.33 Å) bonds. However, there are no such density excesses in the V1—O2 (2.14 Å) and V2—O5 (2.33 Å) regions. Fig. 6 depicts the section of $\Delta\rho$ by the vertical planes through the V atoms along the b axis. The extended regions of the positive $\Delta\rho$ density are observed along the b axis. Splitting of the $\Delta\rho$ maxima at vanadium sites can also be seen in these maps. This splitting could be of some importance as a precursor of the b axis doubling, however, this needs an additional investigation.

Examination of the $\Delta\rho$ maps in the (010) plane (Fig. 5) reveals atomic sheets perpendicular to the mirror plane m in the crystal structure. These sheets run approximately through the sequence of —Na—O6—V2—V1—O5—V3—V3—O5—

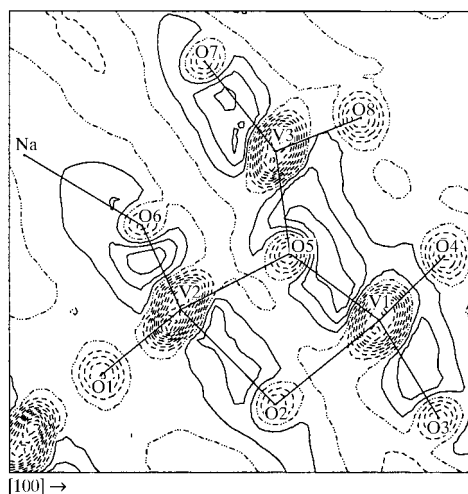
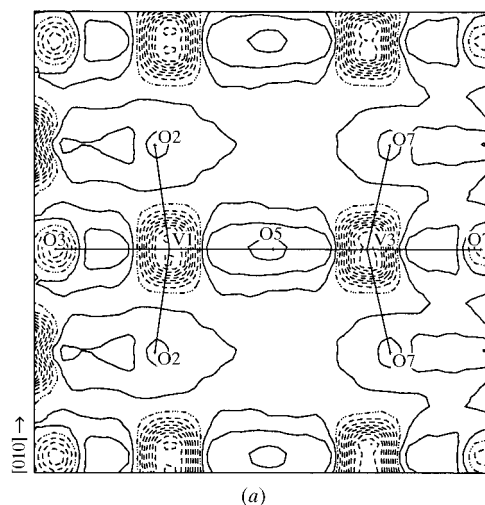


Figure 5
Model deformation ($F_{\text{model}} - F_{\text{sph}}$) electron density maps in the (010) plane in the V_3O_{14} fragment. Contour intervals and map border are as in Fig. 4.

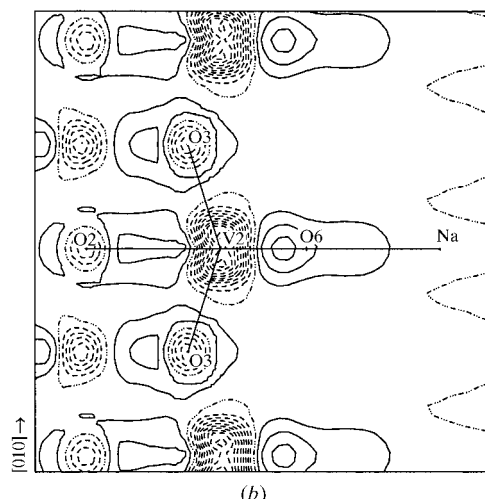
V1—V2—O6—Na— and spread parallel to the y axis through the whole crystal [corresponding crystallographic plane is approximately (20,01)]. There are no ‘covalent’ humps between atoms belonging to two adjacent sheets. The sketch of the sequence for the VO polyhedra approximated by the perfect octahedra in the plane (20,01) is presented in Fig. 7, where the numbers inside the squares specify the corresponding type of V atom.

The relatively strong covalent V—O bonding within the sheets and the absence of such ‘covalent’ bonding between the sheets led to an important question regarding interactions between the sheets in the crystal. They have only the O1 atom in common. The Na atoms also probably play some role in binding sheets together, though no excess (positive or negative) electron density was found around the Na atoms. However, the positive $\Delta\rho$ density near the O6 atom (Fig. 6*b*) is polarized by the positively charged Na^+ cation.

Atomic charges calculated from the monopole populations are given in Table 3. The V charges differ significantly, although the topographies of the $\Delta\rho$ maps are similar near all



(a)



(b)

Figure 6
Model deformation electron density in the plane parallel to the b axis and through (a) V1—V3 and (b) V2—O3. Contour intervals as in Fig. 4. Map borders 5×5 Å.

types of V atoms. The O5 atom, which is the central atom in the V polyhedra junction and acquires electrons from the surrounding chemical bonds, has therefore a relatively large negative charge.

In order to find how extra electrons (from Na atoms) are distributed between the V atoms three models are considered: model 1 – $\text{Na}_2^0\text{V}_{12}^{5+}\text{O}_{30}$, model 2 – $\text{Na}_2^+\text{V}_{12}^{4.86+}\text{O}_{30}$ and model 3 – $\text{Na}_2^+[(\text{V}^{4+}, \text{V}^{5+})_4\text{V}_4''\text{V}_4''']\text{O}_{30}$ (primes denote three independent crystallographic sites of the V atoms). For model 1 the V atoms are all in the pentavalent state and no electron transport exists. If extra electrons are distributed equally among all three V atoms (model 2), then they should have the same valence state of 4.86 for $x = 0.282$, which is 3% less than 5. The same can be said about charges. When only one of the three V atoms accepts electrons then its valence has to be 4.58 (model 3). This corresponds to an 8% reduction of the total atomic charge. However, the difference in charges (Table 3) is noticeably larger than predicted values. Therefore, at this stage it is difficult to identify the V^{4+} atoms in the structure. Goodenough (1970) suggested that V^{4+} ‘prefers’ the V1 site. However, Table 3 shows that this V atom has the intermediate atomic charge and there are no reasons to consider the V1 site as the V^{4+} position. The lowest atomic charge corresponds to the V3 atom, which is located in the most distorted polyhedra.

4.3. Quantum chemistry calculations

An attempt was made to relate the charges of the V atoms with the O polyhedral geometry. Quantum chemistry calculations for the isolated VO_6 octahedra were performed using the restricted Hartree–Fock self-consistent field method within the standard 6-311G* polarized basis set. The GAUSSIAN94 program package was used for our computations.

Two types of octahedra were considered in the calculation: the regular one with the O–V–O distances of 3.6 Å and the irregular one with the V atom shifted from its regular position by 0.2 Å towards either the corner oxygen or along the bisectrix of the O–V–O angle. The Mulliken charges of the V atom were +1.66 and +1.82 e in the first and second cases, respectively. These values can be compared to the charges shown in Table 3 and the agreement is quite reasonable.

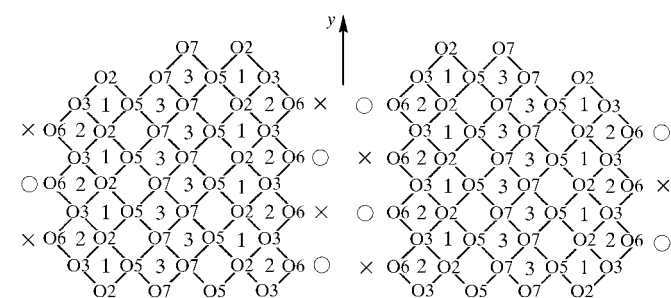


Figure 7
Section of the structure by the approximate (20,01) plane. The V–O polyhedra are approximated by octahedra and the numbers inside them specify the V-atom types. The Na atom sites are marked by circles if occupied and by crosses if empty.

The clusters of octahedra, two with sheared edges and a third arranged as in the crystal structure, were also examined. The V-atom charges appeared to be significantly dependent on the cluster size and symmetry. Therefore, it is not surprising to observe the difference in the charges obtained from the experimental data. The surroundings of V1, V2 and V3 are different in a real bronze structure. Therefore, it can be anticipated that the electronic states of the V atoms in oxygen bronzes are determined not only by the presence of alkali metal atoms, which donate their electrons to form V^{4+} from V^{5+} , but also by the geometry of the vanadium–oxygen coordination octahedra. Further calculations of the vanadium–oxygen bronzes by the different quantum chemistry methods including larger clusters and crystal field modelling may help to clarify the problem.

5. Conclusions

The usually accepted crystal structure of the β phase of sodium vanadium bronze at 9.6 K has been confirmed in all respects.

The deformation electron density ($\Delta\rho$) appeared to be highly anisotropic. The positive $\Delta\rho$ (more covalency) is predominant in the approximate (20,01) plane. This reflects the strong bonds between atoms in the plane, whereas there are no such ‘covalent’ bonds between these planes or sheets. The excess $\Delta\rho$ density in the V–O bonds forms the extended regions of the positive density along the monoclinic b axis. The atomic charges were estimated from the multipole model, however, there is no correlation between the atomic charges and the expected positions for the five- and the four-valence V atoms.

Authors are thankful to Professor G. Chandler for his valuable help in quantum chemistry calculations and to Professor A. N. Vasil’ev for his permanent interest in the work.

References

- Alcock, N. W. (1974). *Acta Cryst.* **A30**, 332–335.
 Becker, P. J. & Coppens, P. (1974). *Acta Cryst.* **A30**, 148–153.
 Canneri, G. & de Pava, V. A. (1936). *Ann. Chim. Appl.* **26**, 560–568.
 Chakraverty, B. K., Sienko, M. J. & Bonnerot, J. (1978). *Phys. Rev. B*, **17**, 3781–3789.
 Gendell, J., Cotts, R. M. & Sienko, M. J. (1962). *J. Chem. Phys.* **37**, 220–225.
 Goodenough, J. B. (1970). *J. Solid State Chem.* **1**, 349–358.
 Hall, S. R., du Boulay, D. J. & Olthof-Hazekamp, R. (1999). Editors. *Xtal3.6 System*. University of Western Australia, Australia.
 Kanai, Y., Kagoshima, S. & Nagasawa, H. (1982). *J. Phys. Soc. Jpn.*, **51**, 697–698.
 Koritsanszky, T., Howard, S., Mallison, P. R., Su, Z., Richter, T. & Hansen, N. (1998). *XD*. Institute of Crystallography, Berlin, Germany.
 Larson, A. C. (1970). *Crystallographic Computing*, edited by F. R. Ahmed, S. R. Hall & C. P. Huber, pp. 291–294. Copenhagen: Munksgaard.
 Maruyama, K. & Nagasawa, H. (1980). *J. Phys. Soc. Jpn.*, **48**, 2159–2160.

- Nagasawa, H., Onoda, M., Kanai, Y. & Kagoshima, Y. (1987). *Synth. Met.* **19**, 971–976.
- Onoda, M. & Nagasawa, H. (1983). *J. Phys. Soc. Jpn*, **52**, 2231–2237.
- Onoda, M. & Nagasawa, H. (1987). *Phys. Status Solidus B*, **141**, 507–515.
- Onoda, M., Takahashi, T. & Nagasawa H. (1982). *Phys. Status Solidus B*, **109**, 793–797.
- Ozerov, R. P. (1954). *Dokl. An. USSR Ser. Phys.* **99**, 93–96 (in Russian).
- Ozerov, R. P. (1955). *Uspechi Chim.* **24**, 951–984 (in Russian).
- Ozerov, R. P. (1957). *Krystallographija*, **2**, 226–232 (in Russian).
- Ozerov, R. P. (1959a). *Krystallographija*, **4**, 201–203 (in Russian).
- Ozerov, R. P. (1959b). *Zh. Neorg. Chim.* **4**, 1047–1054 (in Russian).
- Ozerov, R. P., Gol'der, G. A. & Zhdanov, G. S. (1957). *Krystallographija*, **2**, 217–225 (in Russian).
- Streletsov, V. A. & Zavodnik, V. E. (1989). *Sov. Phys. Crystallogr.* **34**, 824–828.
- Takahashi, T. & Nagasawa, H. (1981). *Solid State Commun.* **39**, 1125–1128.
- Volkov, V. L. (1987). *Inclusion Phases Based on Vanadium Oxides*, p. 179 (in Russian). Sverdlovsk: Academy of Sciences.
- Wadsley, A. D. (1955). *Acta Cryst.* **8**, 695–699.
- Wallis, R. H., Sol, N. & Zylbersztejn, A. (1977). *Solid State Commun.* **23**, 539–542.
- Yamada, H. & Ueda, Y. (1999). *J. Phys. Soc. Jpn*, **68**, 2735–2740.
- Zachariasen, W. H. (1967). *Acta Cryst.* **23**, 558–564.